analytical chemistry

Letter

Cite This: Anal. Chem. 2018, 90, 6357−6361

pubs.acs.org/ac

Pixel Counting of Fluorescence Spots Triggered by DNA Walkers for Ultrasensitive Quantification of Nucleic Acid

Longyi Zhu, Qihui Liu, Bangyu Yang, Huangxian Ju, and Jianping Lei*

State Key Laboratory of Analytical Chemistry for Life Science, School of Chemistry and Chemical Engineering, Nanjing University, Nanjing, Jiangsu 210023, P. R. China

Supporting Information

ABSTRACT: A pixel counting strategy is designed on the basis of DNA walker-triggered fluorescence spots for ultrasensitive detection of nucleic acid. The two-dimensional DNA walker was constructed by hybridization of two types of capture DNAs, which were covalently modified by click chemistry on a glass slide, and dye-labeled hairpin structure (hDNA) as track and swing strand (sDNA) as DNAzyme, respectively. Introduction of target DNA unlocked the sDNA via strand displacement to form the activated DNAzyme, and the latter cut nearby hDNA with Mn^{2+} as cofactor, resulting in fluorescence recovery of dye-labeled hDNA on the substrate due to the separation from the quencher. Meanwhile, the DNAzyme sequence of sDNA was released to cut the next hDNA and, thus, initiated autonomous walking of sDNA for signal amplification. The enhanced fluorescence spots were digitalized as pixels on the basis of DNA walker-built compartments and extracted by a homemade program in MATLAB. The association between fluorescent pixel numbers and DNA concentrations was further proved by a mathematical model and led to an ultrasensitive quantification of nucleic acid with a linear range from 100 fM to 10 pM. The designed pixel counting strategy shows a more sensitive and accurate comparison with conventional methods based on fluorescence intensity or spot counts and provides a new dimension in designing next-type biosensors.

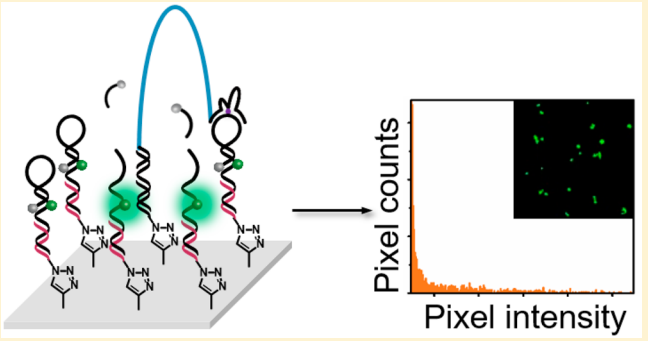

Traditional fluorescence assays are performed in homogeneous solutions by measuring emission intensity,[1] ratiometric fluorescence,[2] fluorescence resonance energy transfer,[3] and time-resolved fluorescence.[4] The main limitation of homogeneous methods is low sensitivity unless coupling with additional signal-amplification strategies. Recently, digital bioassays, which divide reaction volume into many microsized compartments for identical and independent reactions to reduce the background noise,[5] demonstrate high sensitivity in the low target concentration by counting the positive-signal number of compartments.[6−10] However, the fabrication of extrinsic microsized compartments was usually required for generation of digital signals using microwells as barriers and nanoparticles as carriers. Designing a self-built compartment on the surface could directly produce digital signals for developing more convenient and accurate bioassay platforms.

On the other hand, DNA walkers, as the artificial nanomachines, are applied widely in various fields due to the advantages of controllability, specificity, and biocompatibility.[11−14] Upon the movements, DNA walkers can produce large numbers of signal molecules for signal amplification along the multiple dimensional tracks.[15−18] Recently, a new kind of DNA walker with all components covalently conjugated on the nanoparticles can walk continuously in a confined area to release multiple signal strands powered by enzyme cleavage for the signal amplification.[19−21] The autonomous movements of the DNA walkers could light up the fluorescent signals in a confined area, which could be used as an intrinsic microcompartment for digital bioassay. In this work, coupling with DNA walker as initiator and amplifier, a pixel counting strategy was established on the basis of a self-built compartment for sensitive quantification of nucleic acid.

The DNA walker substrate (DW-substrate) was constructed by the covalent assembly of two types of capture DNAs (cDNA 1 and cDNA 2) via click chemistry on the alkynylated glass slides, and this was followed with the hybridization of the fluorescein amidite (FAM)-labeled hairpin structures (hDNA) as the track and blocked swing DNA (sDNA) as the walker strand incorporated a DNAzyme sequence (Scheme 1). Upon the addition of target DNA, the block DNA (bDNA) can be removed from the sDNA via the toehold strand displacement to form the activated DNAzyme.[22] Thus, the autonomous walking of sDNA was initiated by the cleavage of the activated DNAzyme toward hDNA in the presence of Mn^{2+} as cofactor, resulting in fluorescence recovery of FAM on the DW-substrate due to the separation of the black hole quencher-1 (BHQ-1). The "switch on" fluorescent signals of hDNA around the sDNA

Received: March 14, 2018
Accepted: May 17, 2018
Published: May 17, 2018

DOI: 10.1021/acs.analchem.8b01146
Anal. Chem. 2018, 90, 6357−6361

Scheme 1. Schematic Illustration of Establishing Two-Dimensional DNA Walkers and Pixel Counting Strategy for Quantification of Nucleic Acid

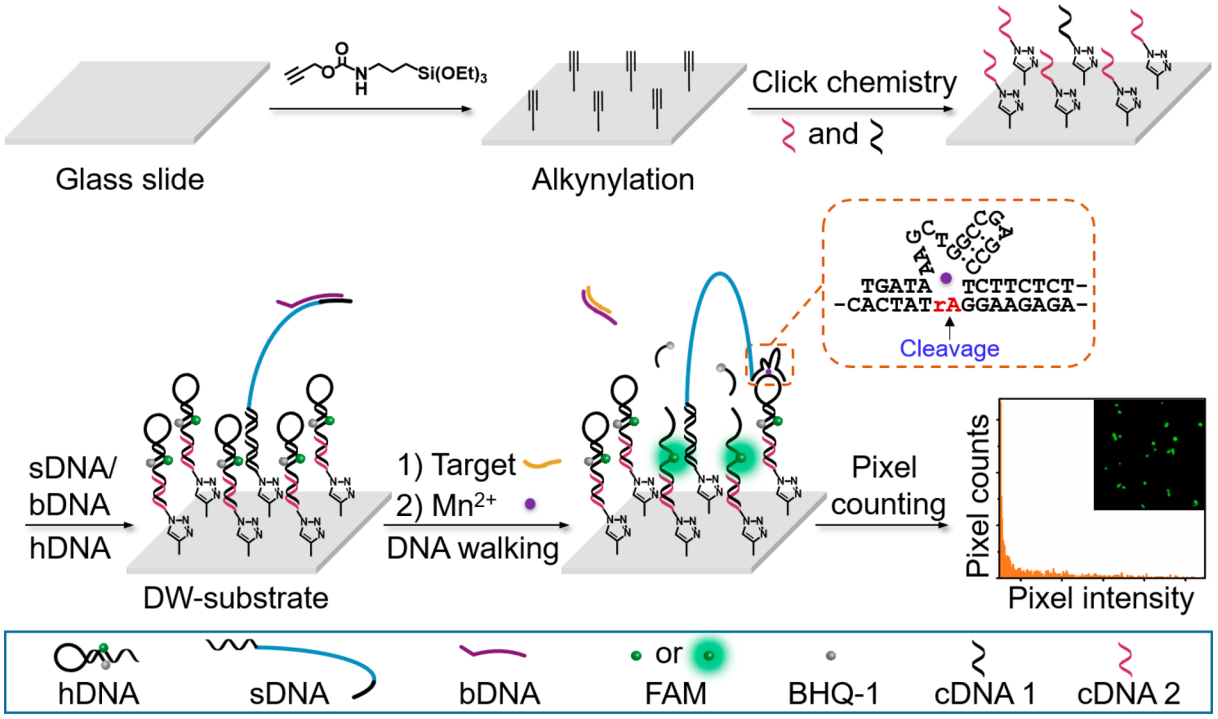

could be observed as fluorescence spots by confocal imaging and digitalized as pixels. As proof of concept, the relationship between fluorescence pixel numbers and DNA concentrations was further proved by a mathematical model. By counting the pixels of fluorescence spots triggered by DNA walkers, an ultrasensitive detection strategy was enabled for quantification of nucleic acid with high accuracy, providing a new data process to improve the analysis performance.

The glass slide was functionalized with *o*-(propargyl)-*n*-(triethoxysilylpropyl)carbamate by vacuum-phase silanization,[23] resulting in the increase of contact angle from ∼17° to ∼61° (Figure 1A). Then, cDNA 1 and cDNA 2 were conjugated onto the alkynylated glass slide by click chemistry,[24] which was verified by X-ray photoelectron spectroscopy (XPS). The peak of phosphorus (P 2p at 134.6 eV) was emerged and the peak of nitrogen (N 1s at 397.7 eV) was stronger after click reaction (Figure 1B), which is attributed to the assembly of azide-modified oligonucleotides on the alkynylated glass slides.[25] The assembly of cDNA 1 and cDNA 2 on the glass slide was confirmed by the reduction of contact angle (Figure S1) and the increase of the roughness (Figure S2).

The strand displacement between the sDNA/bDNA duplex and the target was identified by the polyacrylamide gel electrophoresis (PAGE) image (Figure 1C), which could generate the free end of the sDNA as the activated DNAzyme. Next, the cleavage feasibility of DNAzyme toward the substrate sequence of the hDNA with Mn^{2+} cofactor was verified by fluorescent spectra (Figure 1D). When mixing with DNAzyme and the hDNA in absence of Mn^{2+}, the fluorescent spectrum was similar to that of the hDNA strand. After adding 0.5 mM Mn^{2+} to the mixture, 3.8-fold fluorescent enhancement was obtained, which could be attributed to the dissociation of fluorophore/quencher pair in the hDNA through the efficient cleavage of DNAzyme toward hDNA.

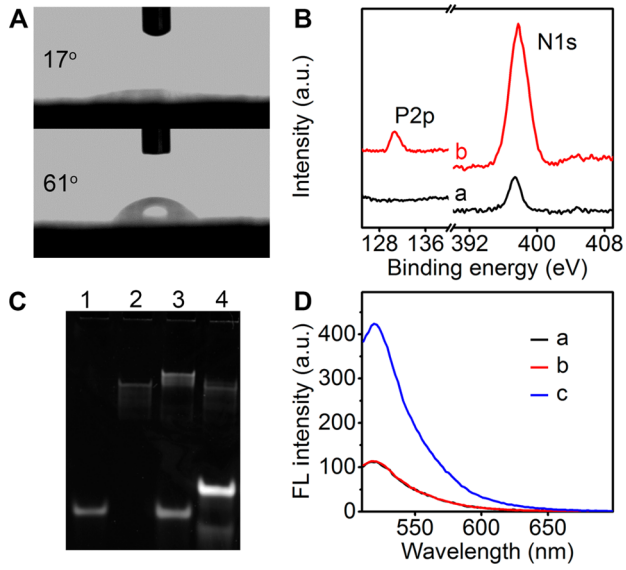

Figure 1. (A) Contact angle of glass slide before (top) and after (bottom) vacuum-phase silanization. (B) XPS spectra before (a) and after (b) conjugation of cDNA on the silanized glass. (C) PAGE image of 1.0 μM bDNA (lane 1), 1.0 μM sDNA (lane 2), mixture of 3.0 μM bDNA + 1.0 μM sDNA (lane 3), and mixture of 3.0 μM target + 1.0 μM sDNA + 3.0 μM bDNA (lane 4). (D) Fluorescent spectra of 1.0 μM hDNA + 0.5 mM Mn^{2+} (a), mixture of 1.0 μM DNAzyme + hDNA without (b) and with (c) 0.5 mM Mn^{2+} in reaction buffer at 25 °C. The excitation wavelength was 494 nm.

The hDNA designed as a hairpin structure was composed of a 7-bp stem and a loop with complete sequence of substrate for DNAzyme, as well as a 15-nt sequence at the 5′ end complementary to cDNA 1 (Table S1, Figures 2A and S3). Time-dependent fluorescence demonstrated that the FL intensity increased with the increase of cleavage time, and the

DOI: 10.1021/acs.analchem.8b01146
Anal. Chem. 2018, 90, 6357−6361

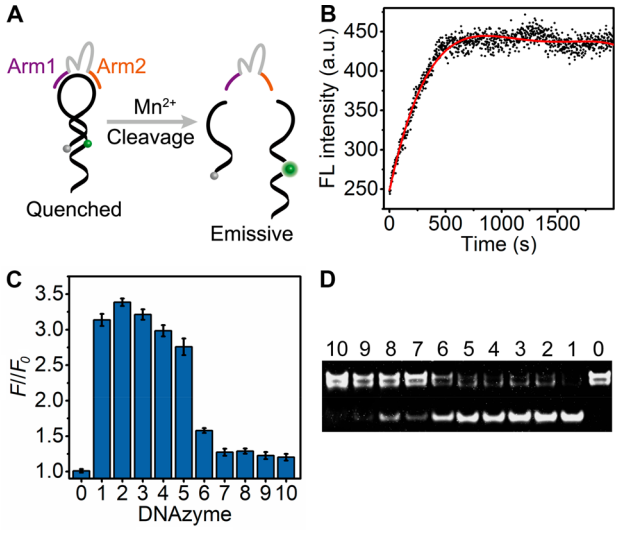

Figure 2. (A) Schematic illustration of hDNA cleaved by DNAzyme and its fluorescent recovery. (B) Time-dependent fluorescence signals for a mixture of 1.0 μM DNAzyme and hDNA in reaction buffer containing 0.5 mM Mn^{2+}. (C) Ratio of fluorescent intensity of 1.0 μM hDNA after (F) and before (F_0) mixing 0.5 mM Mn^{2+} in reaction buffer without (0) and with D(8-8) (1), D(7-7) (2), D(7-6) (3), D(6-7) (4), D(7-5) (5), D(5-7) (6), D(6-5) (7), D(5-6) (8), D(5-5) (9), and D(4-4) (10). (D) PAGE results of 1.0 μM hDNA before (lane 0) and after being mixed with 1.0 μM D(8-8), D(7-7), D(7-6), D(6-7), D(7-5), D(5-7), D(6-5), D(5-6), D(5-5), and D(4-4) corresponding to lanes 1 to 10, respectively, in reaction buffer containing 0.5 mM Mn^{2+}.

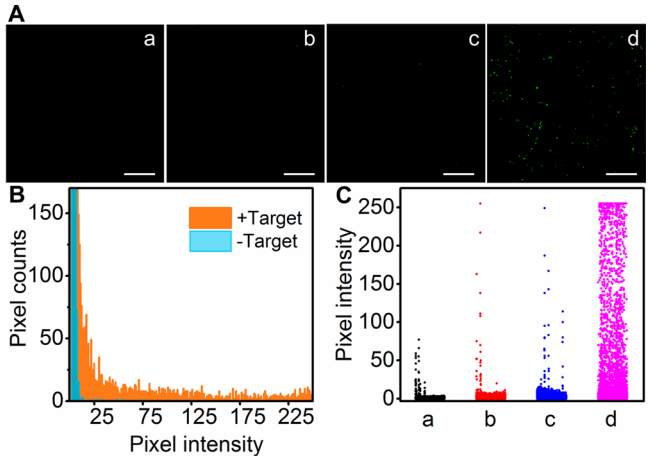

Figure 3. (A) Confocal fluorescent images of DW-substrate before (a) and after addition of 0.5 mM Mn^{2+} (b), 10 pM target DNA (c), and 0.5 mM Mn^{2+} and 10 pM target DNA (d) in reaction buffer. Scale bars: 10 μm. (B) Dependence of pixel counts on fluorescent intensities for DW-substrate in the presence (orange) and absence (blue) of 10 pM target in reaction buffer containing 0.5 mM Mn^{2+}. (C) Distribution of pixel fluorescent intensities for each image in (A).

cleavage turnover time was 500 s (Figure 2B), which was also confirmed by PAGE (Figure S4). To optimize the cleavage efficiency of the hDNA, both arms of DNAzyme were investigated as denoted in D(arm 1-arm 2). As shown in Figure 2C, the ratios of fluorescent intensity of hDNA after (F) and before (F_0) mixing with D(5-7), D(6-5), D(5-6), D(5-5), and D(4-4) were obviously lower than that with D(8-8), D(7-7), D(7-6), D(6-7), and D(7-5) due to less interaction between hDNA and the short arms of DNAzyme,[20,22] which was consistent with PAGE results (Figure 2D). Since the arm length of DNAzyme should be minimized to dissociate from the hDNA and hybridize to the next one for DNA walker, the D(7-5) was the optimized DNAzyme sequence.

Confocal microscopy was used to image the fluorescence spots triggered by DNA walkers on the glass slide with low background (Figure 3A,a). When Mn^{2+} or target was individually added to the DW-substrate, there was also no obvious fluorescence signal with few spots in the image (Figure 3A,b,c). In the presence of both Mn^{2+} and the target, plenty of fluorescence spots were observed in the image (Figure 3A,d), which were attributed to the FAM fluorescence recovery via the activated DNAzyme with Mn^{2+} as the cofactor. When all of the pixel information was extracted from the images by MATLAB (Figure S5),[26] it was found that the pixel intensity of DW-substrate without target was mainly distributed below 11, while the pixel intensity of DW-substrate with target was distributed from 0 to 250 (Figure 3B) and was stable after multiple scans of the images (Figure S6). When the free swing DNA was added on the hDNA-based substrate, the homogeneous fluorescence was observed on the slide (Figure S7).[27] The results suggested that the fluorescence spots on the DW-substrate did not result from the free swing DNA but was triggered by DNA walker.

Moreover, the efficiency of different metal ions has the order: $Mn^{2+} > Mg^{2+} > Zn^{2+} > Pb^{2+} > Ca^{2+} > Ni^{2+}$ (Figure S8). When the pixel intensity below 11 was subtracted as background, a sensitive approach with high accuracy could be enabled in the analysis by pixel counting of DW-substrate with Mn^{2+} as the cofactor (Figure 3C).

The principle of pixel counting of fluorescence spots for detection of nucleic acid is based on digital bioassay theory.[5] In general, on the 2-D surface, every single walker is considered to be identical and an independent compartment and showed either a positive or negative output. Thus, Poisson distribution could be used as the math model. Because the stretch length of sDNA/cDNA 1 complex is estimated to be 66 nm with the stretching area of 13 677 nm^2, the compartment area is set to be 117 × 117 nm^2, which is near the stretching area for accurate pixel counting. As a result, DW-substrate can be theoretically partitioned into 438 × 438 compartments (the same as pixel number). According to Poisson distribution,[5,28] the fraction of positive fluorescent pixels of DNA walkers is proportional to the target concentration.

In pH 7.5 reaction buffer containing 0.5 mM Mn^{2+} at 25 °C (Figures S9–S11), different concentrations of target were added to the DW-substrate modified with 1:1000 of the ratio of sDNA and hDNA (Figures S12 and S13). The fluorescence spots on the DW-substrate increased as the concentration of the target DNA increased (Figure 4A). The average green-channel intensity of each target concentration in Figure 4A cannot be discriminated when target was lower than 0.5 pM (Figure 4B). Moreover, the number of fluorescence spots obtained by ImageJ software in Figure 4A shows the linear relationship with target DNA concentration from 0.2 to 10 pM (Figure 4C). The fluorescent pixel counts increase with the increase of the target DNA concentration ranging from 100 fM to 10 pM with the limit of detection down to 81 fM (Figure 4D), which is much lower than that of other fluorescence methods (Table S2) and the free swing DNA-based method (Figure S14). Moreover, the correlation coefficients of the linear relationship (R^2) of average green-channel intensity and fluorescence spots with logarithm of target concentration are

DOI: 10.1021/acs.analchem.8b01146
Anal. Chem. 2018, 90, 6357−6361

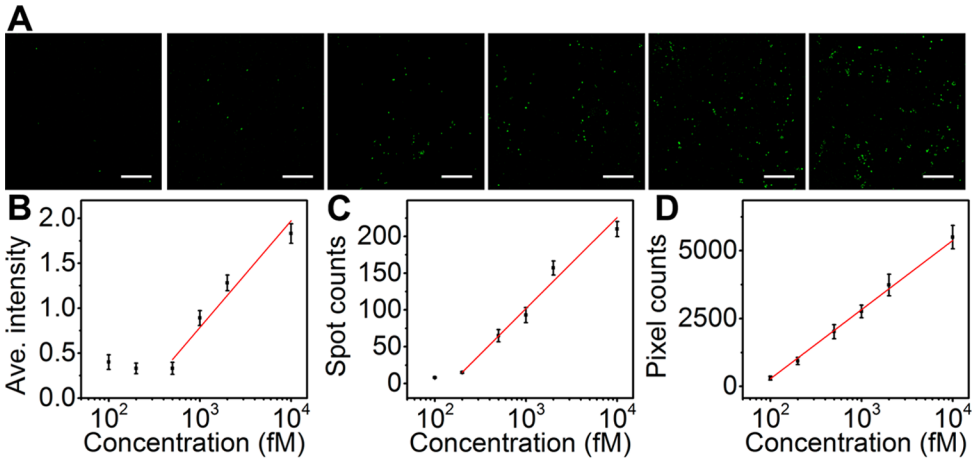

Figure 4. (A) Confocal fluorescent images of DW-substrate at different target concentrations of 0.1, 0.2, 0.5, 1.0, 2.0, and 10.0 pM in reaction buffer containing 0.5 mM Mn^{2+} (from left to right). Scale bars: 10 μm. Dependence of (B) average green-channel intensities, (C) spot counts, and (D) pixel counts on logarithm of target concentration for each concentration in (A).

0.927 and 0.977, respectively, which is lower than 0.997 of the pixel counting strategy. Therefore, the pixel counting strategy with DNA walker demonstrates good performance with better discrimination and accuracy in the detection of trace target.

This work designs a pixel counting strategy based on DNA walkers-triggered fluorescence spots as self-built compartments for sensitive quantification of nucleic acid. By rational design of a hairpin structure with substrate sequence of DNAzyme and fluorophore/quencher pair, we developed a smart 2-D DNA walker as initiator and amplifier on the glass slide. With Mn^{2+} as cofactor, 3.8-fold fluorescent enhancement was obtained through the efficient cleavage of DNAzyme toward hDNA. The fluorescence spots were conveniently digitalized as pixels by a homemade program in MATLAB, and the correlation between concentration of target and the fluorescent pixel numbers was proved by the Poisson distribution model. The designed strategy showed good performance with the detection limit down to femtomole due to the synergy effect of signal amplification of DNA walkers and digital counting strategy. Different from the conventional fluorescence methods based on fluorescence intensity or spot counts, the designed pixel counting strategy shows more sensitivity and accuracy and provides a proof of concept for designing a new type of biosensor.

■ ASSOCIATED CONTENT

Supporting Information

The Supporting Information is available free of charge on the ACS Publications website at DOI: 10.1021/acs.analchem.8b01146.

Materials and reagents, experimental methods including alkynylation of glass slide fabrication of DNA walker substrate (DW-substrate), imaging fluorescence spots on DW-substrate, signal process of fluorescence spots triggered by DNA walkers, DNAzyme performance in solution, and polyacrylamide gel analysis, as well as supplementary figures and tables for characterization of DW-substrate, signal process optimization of detection condition, and assay performance for free swing DNA (PDF)

■ AUTHOR INFORMATION

Corresponding Author

*Phone/Fax: +86-25-89681922. E-mail: jpl@nju.edu.cn (J.L.).

ORCID

Longyi Zhu: 0000-0002-0898-4804
Huangxian Ju: 0000-0002-6741-5302
Jianping Lei: 0000-0002-3594-180X

Notes

The authors declare no competing financial interest.

■ ACKNOWLEDGMENTS

This work was financially supported by the National Key Technologies R&D Program (2016YFC0302500) and National Natural Science Foundation of China (21375060, 21675084, 21635005).

■ REFERENCES

(1) Fateminia, S. M. A.; Mao, Z.; Xu, S. D.; Yang, Z. Y.; Chi, Z. G.; Liu, B. *Angew. Chem., Int. Ed.* **2017**, *56*, 12160−12164.
(2) Shu, T.; Wang, J. X.; Su, L.; Zhang, X. J. *Anal. Chem.* **2016**, *88*, 11193−11198.
(3) Miao, L. Y.; Zhu, C. Z.; Jiao, L.; Li, H.; Du, D.; Lin, Y. H.; Wei, Q. *Anal. Chem.* **2018**, *90*, 1976−1982.
(4) Yang, Y.; Liu, H. L.; Han, M. J.; Sun, B. B.; Li, J. B. *Angew. Chem., Int. Ed.* **2016**, *55*, 13538−13543.
(5) Zhang, Y.; Noji, H. *Anal. Chem.* **2017**, *89*, 92−101.
(6) Li, X. R.; Zhang, D. F.; Zhang, H. M.; Guan, Z. C.; Song, Y. L.; Liu, R. C.; Zhu, Z.; Yang, C. Y. *Anal. Chem.* **2018**, *90*, 2570−2577.
(7) Brault, N. D.; White, A. D.; Taylor, A. D.; Yu, Q. M.; Jiang, S. Y. *Anal. Chem.* **2013**, *85*, 1447−1453.
(8) Nakano, S.; Kanzaki, T.; Nakano, M.; Miyoshi, D.; Sugimoto, N. *Anal. Chem.* **2011**, *83*, 6368−6372.
(9) Leirs, K.; Kumar, P. T.; Decrop, D.; Pérez-Puiz, E.; Leblebici, P.; Kelst, B. V.; Compernolle, G.; Meeuws, H.; Wesenbeeck, L. V.; Lagatie, O.; Stuyver, L.; Gils, A.; Lammertyn, J.; Spasic, D. *Anal. Chem.* **2016**, *88*, 8450−8458.
(10) Wang, L. J.; Yang, Y.; Zhang, C. Y. *Anal. Chem.* **2015**, *87*, 4696−4703.
(11) Qu, X. M.; Zhu, D.; Yao, G. B.; Su, S.; Chao, J.; Liu, H. J.; Zuo, X. L.; Wang, L. H.; Shi, J. Y.; Wang, L. H.; Huang, W.; Pei, H.; Fan, C. H. *Angew. Chem., Int. Ed.* **2017**, *56*, 1855−1858.
(12) Peng, L. C.; Zhang, P.; Chai, Y. Q.; Yuan, R. *Anal. Chem.* **2017**, *89*, 5036−5042.

DOI: 10.1021/acs.analchem.8b01146
Anal. Chem. 2018, 90, 6357−6361

(13) Cha, T. G.; Pan, J.; Chen, H. R.; Robinson, H. N.; Li, X.; Mao, C. D.; Choi, J. H. *J. Am. Chem. Soc.* **2015**, *137*, 9429−9437.
(14) Wang, D. F.; Fu, Y. M.; Yan, J.; Zhao, B.; Dai, B.; Chao, J.; Liu, H. J.; He, D. N.; Zhang, Y.; Fan, C. H.; Song, S. P. *Anal. Chem.* **2014**, *86*, 1932−1936.
(15) Mendoza, O.; Mergny, J. L.; Aimé, J. P.; Elezgaray, J. *Nano Lett.* **2016**, *16*, 624−628.
(16) Yang, X. L.; Tang, Y. N.; Mason, S. D.; Chen, J. B.; Li, F. *ACS Nano* **2016**, *10*, 2324−2330.
(17) He, M. Q.; Wang, K.; Wang, W. J.; Yu, Y. L.; Wang, J. H. *Anal. Chem.* **2017**, *89*, 9292−9298.
(18) Li, W.; Wang, L.; Jiang, W. *Chem. Commun.* **2017**, *53*, 5527−5530.
(19) Zhang, H. Q.; Lai, M. D.; Zuehlke, A.; Peng, H. Y.; Li, X. F.; Le, X. C. *Angew. Chem., Int. Ed.* **2015**, *54*, 14326−14330.
(20) Peng, H. Y.; Li, X. F.; Zhang, H. Q.; Le, X. C. *Nat. Commun.* **2017**, *8*, 14378.
(21) Zhang, Y.; Wang, L. X.; Luo, F.; Qiu, B.; Guo, L. H.; Weng, Z. Q.; Lin, Z. Y.; Chen, G. N. *Chem. Commun.* **2017**, *53*, 2910−2913.
(22) Song, P. S.; Xiang, Y.; Xing, H.; Zhou, Z. J.; Tong, A. J.; Lu, Y. *Anal. Chem.* **2012**, *84*, 2916−2922.
(23) Meng, X.; Hu, J. J.; Chao, Z. C.; Liu, Y.; Ju, H. X.; Cheng, Q. *ACS Appl. Mater. Interfaces* **2018**, *10*, 1324−1333.
(24) Yehl, K.; Mugler, A.; Vivek, S.; Liu, Y.; Zhang, Y.; Fan, M. Z.; Weeks, E. R.; Salaita, K. *Nat. Nanotechnol.* **2016**, *11*, 184−190.
(25) Jhaveri, S. B.; Carter, K. R. *Langmuir* **2007**, *23*, 8288−8290.
(26) Qian, R. C.; Cao, Y.; Zhao, L. J.; Gu, Z.; Long, Y. T. *Angew. Chem., Int. Ed.* **2017**, *56*, 4802−4805.
(27) Li, C.; Li, X. X.; Wei, L. M.; Liu, M. Y.; Chen, Y. Y.; Li, G. X. *Chem. Sci.* **2015**, *6*, 4311−4317.
(28) Bertsekas, D. P.; Tsitsiklis, J. N. In *Introduction to Probability*, 2 ed.; Athena Scientific: Belmont, MA, 2008; p 307.

DOI: 10.1021/acs.analchem.8b01146
Anal. Chem. 2018, 90, 6357−6361